



⟨Research Article⟩

## Fecal supernatant from renalase gene knockout mice weakens the AKT/JNK pathway to decrease the expression of *Pc1/3* and Boc-Arg-Val-Arg-Arg-MCA cleaving activity in STC-1 cell line

Hui Fang<sup>1</sup>, Kai Aoki<sup>2,3</sup>, Katsuyuki Tokinoya<sup>3,4</sup>, Yasuko Yoshida<sup>5</sup>, Masato Yonamine<sup>1,2</sup>, Yasushi Kawakami<sup>2</sup> and Kazuhiro Takekoshi<sup>2,\*</sup>

**Summary** Prohormone converting enzyme 1/3 (*Pc1/3*) is known to lower glucose levels by elevating the production of glucagon-like peptide 1. Obesity and type 2 diabetes (T2D) are often accompanied by dysfunction of enteroendocrine L cells, inactivity, and low expression of *Pc1/3* and are related to the microbiota composition. The renalase gene (*Rnls*) has been reported to increase the risk of T2D. Recently, we reported that *Rnls* knockout (*Rnls*<sup>-/-</sup>) altered the microbiota composition; however, its effects on enteroendocrine L cells are unknown. In this study, we aimed to reveal the effects of *Rnls*<sup>-/-</sup> mice fecal supernatant stimulations on enteroendocrine L cell functions in vitro. We co-cultured STC-1 cell line, a model of enteroendocrine L cells with fecal supernatants extracted from wild-type (*Rnls*<sup>+/+</sup>) and *Rnls*<sup>-/-</sup> mice. We assessed the effects of fecal supernatant on cell proliferation, the underlying pathway, the mRNA expression of *Pc1/3* and the enzymatic hydrolysis activity of Boc-Arg-Val-Arg-Arg-MCA (a substrate of hydrolyzing enzyme family included *Pc1/3*). STC-1 cells co-cultured with fecal supernatant from *Rnls*<sup>+/+</sup> mice effectively promoted cell proliferation via upregulation of the AKT/JNK pathway and elevated mRNA expression of *Pc1/3*. Moreover, we found that STC-1 cells co-cultured with fecal supernatant from *Rnls*<sup>+/+</sup> mice effectively increased Boc-Arg-Val-Arg-Arg-MCA cleaving activity. Conversely, fecal supernatants from *Rnls*<sup>-/-</sup> mice failed to activate the AKT/JNK pathway and reduced the mRNA expression of *Pc1/3* and the enzymatic hydrolysis activity of Boc-Arg-Val-Arg-Arg-MCA. In conclusion, *Rnls* knockout impaired L cell function by altering the gut microbiota-derived metabolites, which may accelerate T2D progression.

**Key words:** *Rnls*<sup>-/-</sup> mice, Fecal supernatant, STC-1 cell, Prohormone converting enzyme 1/3, AKT/JNK pathway

### 1. Introduction

Diabetes, a chronic metabolic disease, leads to several life-threatening complications and deteriorates

the quality of life of patients worldwide<sup>1</sup>. Prolonged hyperglycemia is a classic characteristic of type 2 diabetes (T2D)<sup>2-4</sup>; therefore, effective regulation of glucose metabolism has become the key breakthrough point in treating T2D<sup>5,6</sup>. In 1985, researchers discovered

<sup>1</sup> Graduate School of Comprehensive Human Sciences, University of Tsukuba, 1-1-1 Tennodai, Tsukuba, Ibaraki 305-8577, Japan.

<sup>2</sup> Division of Clinical Medicine, Faculty of Medicine, University of Tsukuba, 1-1-1Tennodai, Tsukuba, Ibaraki 305-8577, Japan.

<sup>3</sup> Research Fellow of the Japan Society for the Promotion of Science, 5-3-1 Kojimachi, Chiyoda-ku, Tokyo, 102-0083, Japan.

<sup>4</sup> Department of Health Promotion Sciences, Graduate School of Human Health Sciences, Tokyo Metropolitan University, 1-1 Minami-Osawa, Hachioji-shi, Tokyo, 192-0397, Japan.

<sup>5</sup>Department of Clinical Laboratory Science, Faculty of Health Sciences, Tsukuba International University, 6-20-1 Manabe, Tsuchiura, Ibaraki 300-00051, Japan.

\*Corresponding author: Kazuhiro Takekoshi, Division of Clinical Medicine, Faculty of Medicine, University of Tsukuba, 1-1-1Tennodai, Tsukuba, Ibaraki 305-8577, Japan.  
E-mail: k-takemd@md.tsukuba.ac.jp

Received for Publication: October 4, 2022

Accepted for Publication: November 18, 2022

an incretin called glucagon-like peptide 1 (GLP-1)<sup>7</sup>. It is produced by the specific cleavage of proglucagon under the action of prohormone converting enzyme 1/3 (Pc1/3) in enteroendocrine large granule cell<sup>8</sup>. GLP-1 interacts with the GLP-1 receptor on pancreatic islet  $\beta$  cells to activate intracellular cyclic adenosine monophosphate, initiating the transcription of the insulin gene to induce insulin secretion and lower glucose levels in the circulatory system<sup>8-10</sup>. Therefore, enteroendocrine L cells and the expression and activity of Pc1/3 play important roles in the regulation, development, and treatment of T2D.

The gut is the habitat of the microbiota colonizing the gastrointestinal tract and endocrine L cells<sup>11-13</sup>. Previous studies have revealed that colonized microbiota and their metabolites increase the number of enteroendocrine L cells to improve glucose homeostasis<sup>14</sup>. In addition, probiotics, such as *Lactobacillus* and *Bifidobacterium* strains, enhance insulin secretion and exert glucose regulatory effects by upregulating the activities of Pc1/3<sup>15</sup>. The gut microbiota-derived metabolites are also involved in glucose regulation in different ways. For example, short-chain fatty acids (SCFAs) increase enteroendocrine L cell density and promote GLP-1 production via the G protein-coupling receptor<sup>16,17</sup> wherein secondary bile acids promote L cell differentiation via 5-hydroxytryptamine (5-HT) signaling<sup>18</sup>. Furthermore, an adaptive relationship between the host and gut microbiota has also been reported<sup>19</sup>. In other words, the host gene can affect the gut microbiota composition and their metabolites, and the gut microbiota and their metabolites participate in maintaining the fitness of the host.

Renalase was first discovered in 2005 as a flavo-protein oxidase, synthesized in the kidney<sup>20</sup>. With research advancements, single nucleotide polymorphisms of *Rnls* were found that a closely correlation with an increasing risk of diabetes and complications<sup>21-23</sup>. It has also been reported to exert anti-inflammatory and antioxidative effects and is involved in gene transcription<sup>24-26</sup>. Our previous study reported that *Rnls* is highly expressed in the intestinal crypt for anti-oxidation<sup>26</sup>. Recently, we have demonstrated that *Rnls* knockout (*Rnls*<sup>-/-</sup>) resulted in the remodeling of the gut microbiota<sup>27</sup>. However, the relationship between

*Rnls*, gut microbiota, and enteroendocrine L cell function is still unclear. Therefore, in this study, we aimed to determine the effect of dysbiosis of gut microbiota and metabolites on the biological activity of endocrine L cells in *Rnls*<sup>-/-</sup> mice.

## 2. Materials and Methods

### Mice

Fifteen male B6,129S1-Rnlstm1Gvd/J mice (*Rnls*<sup>-/-</sup> mice, four-week-old) and 15 healthy male C57BL/6J mice (wild-type mice (*Rnls*<sup>+/+</sup>); four-week-old) were obtained from Jackson Laboratory (CA, USA). All mice were housed in microisolator cages at 23-26°C and humidity of 60% with a 12-h light/dark cycle and free access to a normal diet (ND; Cat#MF; Oriental Yeast, Itabashi, Tokyo, Japan) and sterile water, five mice in one cage. After 1 week of acclimatization to the environment, the mice were divided into *Rnls*<sup>-/-</sup>-ND (n = 15) and *Rnls*<sup>+/+</sup>-ND (n = 15) groups and mice in each group were numbered from one to fifteen, fed with ND throughout the experimental period (8 weeks). The guidelines of the Animal Care Committee of the University of Tsukuba (approval number: 21-027) were followed during the whole animal experimental procedures.

### Fecal supernatant preparation

Thirty clean and sterile microisolator cages were taken without bedding substrate and numbered the cage according to the grouping of mice. Afterwards, mice in each group were placed in correspondingly numbered cages (one mouse per cage) and allowed to defecate naturally. After 5-10 minutes, 3-5 droppings were visible in each cage. The feces were then picked up with sterile forceps and placed in two pre-labelled 10 ml centrifuge tubes (marked as *Rnls*<sup>+/+</sup>-ND and *Rnls*<sup>-/-</sup>-ND group). By this way, samples of fresh feces from *Rnls*<sup>+/+</sup>-ND and *Rnls*<sup>-/-</sup>-ND groups (1 g from each group) were enough collected, and each mouse contributed. After that, dissolved in 5 mL phosphate buffer (PBS: 2.7 mmol/L KCl, 1.76 mmol/L KH<sub>2</sub>PO<sub>4</sub>, 137 mmol/L NaCl, and 10 mmol/L Na<sub>2</sub>HPO<sub>4</sub>) and homogenized

on ice. Subsequently, the homogenized solution was centrifuged (10000 ×g, 10 min, 4°C) as described in previous studies<sup>28,29</sup>. Supernatants were collected, and coarse particles and bacteria were removed by filtration using a 0.22-µm filter (Millex-GV, Merck Millipore Limited, Tullagreen, Ireland.)<sup>28,29</sup>.

#### Cell culture

STC-1 cell line was purchased from American Type Culture Collection (CRL-3254™, ATCC, VA, USA). Dulbecco's modified Eagle's medium (DMEM; high glucose with L-glutamine; Cat#11965092, Thermo Fisher Scientific, MA, USA) with 10% fetal bovine serum (FBS; Cat#CCP-FBS-BR-500, Cosmo Bio, Tokyo, Japan), 100 U/mL penicillin, and 100 mg/mL streptomycin were used for cell culture. Cells were grown at 37°C and 5% CO<sub>2</sub>.

#### Cell viability assay

1.5 × 10<sup>5</sup> cells/well were seeded and those 12-well plates were stimulated with 50 µL fecal supernatant (from *Rnls*<sup>+/+</sup> and *Rnls*<sup>-/-</sup> mice) or 50 µL PBS plus 2% FBS DMEM (1.15 mL) after overnight culture in DMEM. Cell viability was measured using the resazurin assay, as described previously<sup>30</sup>. Briefly, Medium (1 mL) containing 0.004% resazurin (Cat#R0203, Tokyo Chemical Industry, Tokyo, Japan) was added to each well after 48 h of stimulation, and incubated for 3 h at 37°C. Subsequently, a 96-well black plate was used for holding medium (100 µL) from each well. The fluorescence intensity of the medium was measured at 590 nm emission and 569 nm excitation wavelengths using Varioskan LUX (Thermo Fisher Scientific, MA, USA). All treatments were performed in triplicates.

#### Western blotting

5 × 10<sup>5</sup> cells/well were seeded in 6-well plates, and at 85–90% confluence, the culture medium was changed to 2% FBS DMEM. STC-1 cells were stimulated with 100 µL fecal supernatant or 100 µL PBS plus 2% FBS DMEM (2.3 mL). The cells were harvested for protein and RNA analyses after 48 h of stimulation. All treatments were performed in triplicates.

Cells were scraped from plates into ice-cold NP40 lysis buffer (1% NP40, 150 mmol/L NaCl, 50 mmol/L Tris-HCl (pH 7.5)) that included a protease inhibitor cocktail (Cat#25955-24, Nacalai Tesque, Kyoto, Japan) and phosphate inhibitor (Cat#4906845001, Roche, Basel, Switzerland) tablets in a microtube. The supernatants of the protein lysates were moved to new microtubes after centrifuged at 12,000 ×g for 15 min at 4°C. Subsequently, using a BCA assay kit (Cat#T9300A, Takara Bio, Tokyo, Japan) to detect the protein concentrations following the manufacturer's instructions. The protein lysate (2 mg/mL) were adjusted and mixed with 2× loading buffer including 2-mercaptoethanol and denatured at 95°C for 5 min. Afterward, sodium dodecyl sulfate-polyacrylamide gel electrophoresis (10%) was performed at 120 V for 90 min for separation the prepared sample. Subsequently, a polyvinylidene fluoride membrane was used for protein transmembrane by an overnight wet transfer method at 25 V, 4°C. TBS-T buffer (50 mmol/L Tris-HCl, 150 mmol/L NaCl, 0.05% Tween 20, pH 7.6) containing 5% skim milk was used for blocking the membrane for 60 min, and then washing with a TBS-T buffer for three times (5 min/time). The membrane was incubated with the primary antibody listed in Table 1 with overnight gentle shaking at 4°C.

Table1 List of antibodies

Antibody name	Company and code	Dilution
P44/42	Cell signaling technology, #4695	1:1000
p-P44/42	Cell signaling technology, #4377	1:1000
SAPK/JNK	Cell signaling technology, #9252	1:1000
p-SAPK/JNK	Cell signaling technology, #4668	1:1000
AKT	Cell signaling technology, #9272	1:1000
p-AKT	Cell signaling technology, #9271	1:1000
GAPDH	Santaacruz Biotechnology, sc-365062	1:1000

The next day, the membrane was washed with TBS-T buffer three times (5 min/time), then incubated with the secondary antibody: anti-mouse IgG (1:5000, #7076, Cell Signaling Technology, MA, USA) and anti-rabbit IgG (1:5000, #7074, Cell Signaling Technology, MA, USA) with gentle shaking at room temperature for 60 min. After three times washing with TBS-T buffer, a chemiluminescence reagent (WSE-7120, EzWestLumi Plus, ATTO, Tokyo, Japan) was used for visualizing the target protein bands on FUSION FX7.EDGE (Vilber Lourmat, Marne-la-Vallée, France) and saved as TIFF images. Finally, using ImageJ Fiji (version Java 8, Bethesda, USA) to quantify the intensity of the bands.

#### Gene expression analysis

STC-1 cells were cultured and harvested as described in the previous section. Afterward, Sepasol-RNA I Super G (Cat#09379-55, Nacalai Tesque, Kyoto, Japan) was used for RNA extraction, following the manufacturer's instructions to quantify the expression of *Pc1/3* in STC-1 cells stimulated with different fecal supernatants. The concentration of extracted total RNA was adjusted to 100 ng/ $\mu$ L with Milli-Q water. Using the PrimeScript RT Master Mix (Cat#RR036A, Takara Bio, Tokyo, Japan) and according to the manufacturer's instructions, cDNAs were prepared. Diluting cDNAs to 10 times by MilliQ water for the quantitative polymerase chain reaction (qPCR). The reaction volume of qPCR comprised 5  $\mu$ L master mix (Cat#RR820S, TB green Premix Eq II, Takara Bio, Tokyo, Japan), 0.1  $\mu$ L primer solution (10  $\mu$ mol/L forward and reverse each), 2  $\mu$ L template, and 2.8  $\mu$ L Milli-Q water. The QuantStudio 5 Real-Time PCR System (Thermo Fisher Scientific, MA, USA) was used for monitoring the amplification. Thermal cycling conditions are as follows: one cycle at 95°C for 5 min, subsequently 40 cycles at 95°C for 3 s, and 60°C for 30 s for melting curve analysis. The primers are as follows: GAPDH (forward sequence 5'-GGAAACCCATCACCATCTTC-3', reverse sequence 5'-GTGGTTCACCCATCACAA-3'); *Pc1/3* (forward sequence

5'-GCEAAGAGGCAGTTTGTTAATGA-3', reverse sequence 5'-TGATTTCAAGTGATCCAATCTG-3'). All qPCR assays were conducted in duplicate. Relative gene expression was normalized by GAPDH, and analyzed it using quantification cycle (Cq) values and the two delta-delta CT ( $2^{-\Delta\Delta CT}$ ) method.

Analysis of the enzymatic hydrolysis activity of Boc-Arg-Val-Arg-Arg-MCA

For the assessment of the enzymatic hydrolysis activity of t-Butyloxycarbonyl-L-arginyl-L-valyl-L-arginyl-L-arginine 4-methylcoumaryl-7-amide (Boc-Arg-Val-Arg-Arg-MCA), STC-1 cells were seeded in 12-well plates at a density of  $1.5 \times 10^5$  cells. At 85–90% confluence, the culture medium was changed to 2% FBS DMEM. STC-1 cells were stimulated with 50  $\mu$ L mice fecal supernatant or 50  $\mu$ L PBS plus 2% FBS DMEM (1.15 mL). All treatments were performed in triplicates. Co-cultured cells at 0, 6, 12, 24, 36, 48h were scraped from plates into ice-cold NP40 lysis buffer (1% NP40, 150 mmol/L NaCl, 50 mmol/L Tris-HCl (pH 7.5)) that included a protease inhibitor cocktail (Cat#25955-24, Nacalai Tesque, Kyoto, Japan) and phosphate inhibitor (Cat#4906845001, Roche, Basel, Switzerland) tablets in a microtube. The supernatants of the protein lysates were moved to new microtubes after centrifuged at  $12,000 \times g$  for 15 min at 4°C. Subsequently, using a BCA assay kit (Cat#T9300A, Takara Bio, Tokyo, Japan) to detect the protein concentrations following the manufacturer's instructions. The protein lysate concentration was adjusted to 3 mg/mL for further study.

*Pc1/3* is the mammalian homologs of the KEX2 proteinase, while KEX2 included other processing endopeptidases, such as *Pc2*, *Pc4*, *Pc4* and so on<sup>8</sup>. The encoded enzymes have been proved to correctly process some protein or peptide precursors into their mature forms by cleaving mainly after basic amino acid pairs such as Lys-Arg and Arg-Arg. Hence, the peptide called Boc-Arg-Val-Arg-Arg -MCA (3155-V, Peptide Institute Inc, Osaka, Japan) was used for analyzed the enzyme activity. Fifteen microgram (5 $\mu$ L) protein lysates as the enzyme source were added to the assay buffer (5  $\mu$ L, 4 mmol/

L Boc-Arg-Val-Arg-Arg-MCA and 40  $\mu$ L, 0.1% bovine serum albumin-1mmol/L  $\text{CaCl}_2$ ). The mixture was incubated at 37°C for 30 min, and the reaction was stopped by adding 200  $\mu$ L, 1 mol/L acetic acid. Finally, the fluorescence intensity was measured at emission 460 nm/excitation 380 nm<sup>31</sup>. One unit (1U) of enzyme activity is defined as the fluorescence intensity increased per 0.01 into the corresponding product in 30 min at 37°C.

#### Statistical analyses

Using GraphPad Prism version 8 software (GraphPad Software, CA, USA), one-way analysis of variance (ANOVA) with Tukey's test was used for comparing the difference among the three groups, and an unpaired t-test was used for comparing the difference between the two groups. The mean  $\pm$  standard deviation was selected for exhibiting data. Statistically significant was defined as P values of < 0.05.

### 3. Results

Fecal supernatant from *Rnls*<sup>+/+</sup> mice effectively promotes the cell proliferation of STC-1 cell line

As shown in Fig. 1, the proliferation of STC-1 cells co-cultured with fecal supernatants for 48 h was elevated compared to that in those co-cultured with PBS (*Rnls*<sup>+/+</sup>-ND group vs. PBS group, P < 0.01; *Rnls*<sup>-/-</sup>-ND group vs. PBS group, P < 0.05).

Fecal supernatant from *Rnls*<sup>+/+</sup> mice effectively activated the AKT/JNK signaling pathway in STC-1 cells

To further elucidate the role of metabolites in L cell activation, we incubated fecal supernatant with STC-1 cells and analyzed the classic signaling pathway, such as phosphorylation level of SAPK/JNK (p-SAPK/JNK), AKT (p-AKT) and P44/42 (p-P44/42). STC-1 cells co-cultured with the fecal supernatant from *Rnls*<sup>+/+</sup> mice had high expression of p-SAPK/JNK and p-AKT relative to that of GAPDH (Fig. 2A, B). However, there was no difference in p-P44/42 expression among the three groups (Fig. 2B). In addition, the ratio of p-P44/42/P44/42,

p-AKT/AKT, and p-SAPK/JNK/SAPK/JNK demonstrated similar results (Fig 2C–E). STC-1 cells co-cultured with the fecal supernatant showed an increased p-AKT/AKT ratio, while there was no difference in the ratio of p-P44/42/P44/42 (Fig 2C, E). In addition, STC-1 cells co-cultured with the fecal supernatant from *Rnls*<sup>-/-</sup> mice showed a decreased p-SAPK/JNK/SAPK/JNK ratio compared to *Rnls*<sup>+/+</sup> mice (Fig 2D).

Fecal supernatant from *Rnls*<sup>+/+</sup> mice elevates the mRNA expression of *Pcl/3* in STC-1 cell line

Quantification of the mRNA expression of *Pcl/3* demonstrated that STC-1 cells co-cultured with the fecal supernatant from *Rnls*<sup>+/+</sup> mice showed elevated mRNA expression of *Pcl/3* compared to those co-cultured with fecal supernatant from *Rnls*<sup>-/-</sup> mice and PBS. STC-1 cells co-cultured with the fecal supernatant from *Rnls*<sup>-/-</sup> mice did not influence the mRNA expression of *Pcl/3* (Fig. 3).

The fecal supernatant enhanced the enzymatic hydrolysis activity of Boc-Arg-Val-Arg-Arg-MCA in STC-1 cells with a time-dependent manner.

To understand the effects of fecal supernatant stimulation on the enzymatic hydrolysis activity of Boc-Arg-Val-Arg-Arg-MCA in STC-1 cells, we monitored the changes in the enzymatic hydrolysis activity of Boc-Arg-Val-Arg-Arg-MCA over time. The findings demonstrated that the enzymatic hydrolysis activity of Boc-Arg-Val-Arg-Arg-MCA was time-dependent, increasing from 0 to 12 h and decreasing after that till 48 h, and it reached the peak in each group at 12 h (Fig. 4A, B). This result suggested that the enzymatic hydrolysis activity of Boc-Arg-Val-Arg-Arg-MCA was unrelated to the stimulation factors. Moreover, the enzymatic hydrolysis activity of Boc-Arg-Val-Arg-Arg-MCA was the highest in STC-1 cells stimulated with fecal supernatant from *Rnls*<sup>+/+</sup> mice (Fig. 4C).

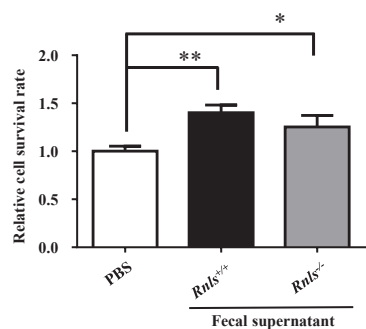


Fig. 1. Effects of fecal supernatants from *Rnls*<sup>+/+</sup> and *Rnls*<sup>-/-</sup> mice on cell proliferation of STC-1 cell line. Relative cell survival rate. STC-1 cells were stimulated with different fecal supernatants for 48 h. Asterisks indicate significant differences (\*P < 0.05, \*\*P < 0.01 vs. PBS). Data are shown as the mean ± standard deviation (SD); n = 3 in each group.

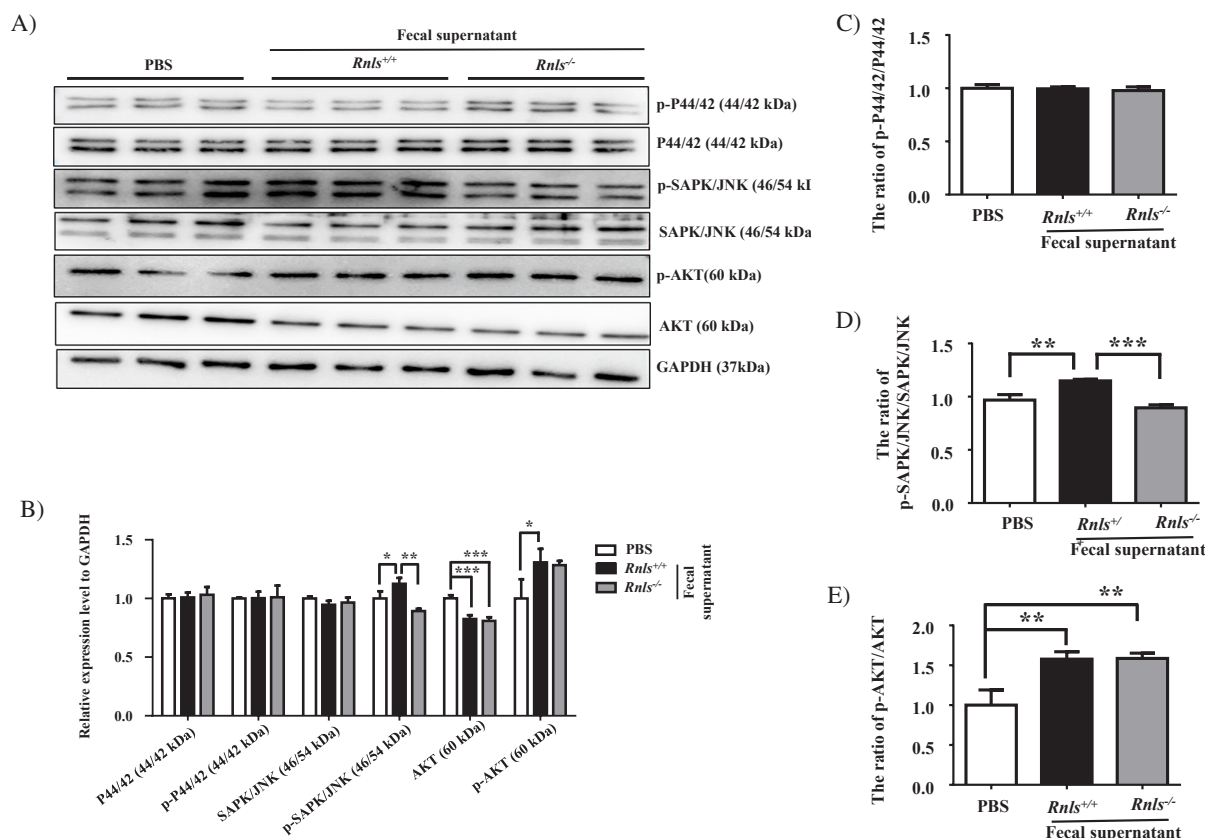


Fig.2. Effects of fecal supernatant from *Rnls*<sup>+/+</sup> and *Rnls*<sup>-/-</sup> mice on Akt/JNK signaling pathway activation in STC-1 cell line. The protein expression levels of p-P44/42, P44/42, p-SAPK/JNK, SAPK/JNK, p-AKT and AKT were analyzed using western blotting after stimulating STC-1 cells with different fecal supernatants for 48 h. (A) Representative western blot images, (B) The protein expression of p-P44/42, P44/42, p-SAPK/JNK, SAPK/JNK, p-AKT and AKT relative to GAPDH, the ratio of (C) p-P44/42/P44/42, (D) p-SAPK/JNK/ SAPK/JNK, and (E) p-AKT/AKT. \*P < 0.05, \*\*P < 0.01, \*\*\*P < 0.001 were considered as significant difference among the three groups. Data are shown as the mean ± SD; n = 3 in each group.

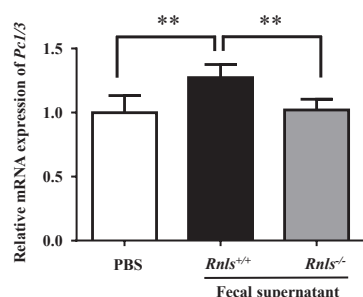


Fig. 3. Effects of fecal supernatants from *Rnls*<sup>+/+</sup> and *Rnls*<sup>-/-</sup> mice on the mRNA expression of *Pcl/3* in STC-1 cell line. STC-1 cells were stimulated with different fecal supernatants for 48 h, and the mRNA expression of *Pcl/3* was analyzed using qPCR post-stimulation. \*\*P < 0.01 vs. fecal supernatant from *Rnls*<sup>+/+</sup> mice. Data are shown as the mean ± SD; n = 3 in each group.

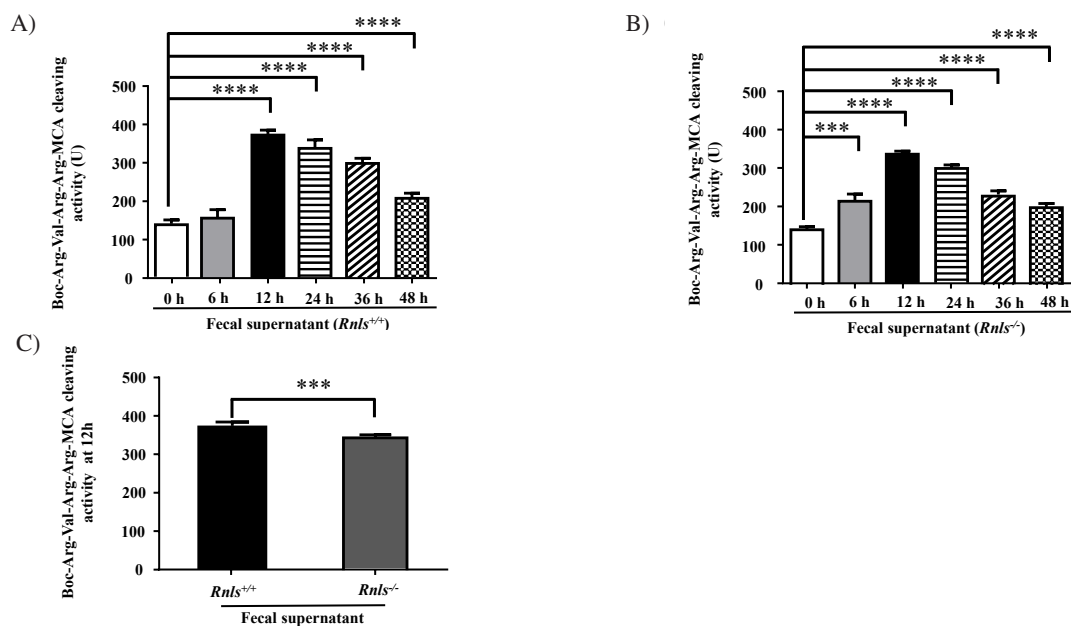


Fig. 4. Effects of fecal supernatants from *Rnls*<sup>+/+</sup> and *Rnls*<sup>-/-</sup> mice on the enzymatic hydrolysis activity of Boc-Arg-Val-Arg-Arg-MCA in STC-1 cell line. The enzymatic hydrolysis activity of Boc-Arg-Val-Arg-Arg-MCA in STC-1 cells co-cultured with fecal supernatants from *Rnls*<sup>+/+</sup> (A) and *Rnls*<sup>-/-</sup> (B) mice exhibited a time-dependent behavior. (C) the enzymatic hydrolysis activity of Boc-Arg-Val-Arg-Arg-MCA in STC-1 cells after 12 h co-culturing with different fecal supernatant. (A, B) \*\*\*\*P < 0.0001 vs. 0 h; (C) \*\*\*P < 0.001 vs. fecal supernatant from *Rnls*<sup>+/+</sup> mice; Data are shown as mean ± SD; n = 3 in each group.

#### 4. Discussion

In this study, the underlying metabolites of gut microbiota from *Rnls*<sup>+/+</sup> and *Rnls*<sup>-/-</sup> mice induced different endocrine L cell functions was demonstrated. Gut homeostasis is considered a key factor in maintaining endocrine L cell function and is influenced by the environment and host genetics<sup>11-13</sup>. One of our recent studies showed that *Rnls* plays the critical part in remodeling the gut microbiota<sup>27</sup>. The elevated ratio of Firmicutes/Bacteroidetes and decreased abundance of *Bifidobacterium pseudolongum* in *Rnls*<sup>-/-</sup> mice indicate an increased risk of T2D<sup>32</sup> and glycolipid dysfunction<sup>33,34</sup>. Moreover, our previous study demonstrated that *Rnls* knockout accelerates the progression of nonalcoholic steatohepatitis; conversely, increased *Rnls* expression effectively decreased oxidative injury in Caco-2 cells<sup>25,26</sup>. These results indicate the protective effects of *Rnls*. In this study, we co-cultured STC-1 cells with the extracted fecal supernatant with abundant metabolites of microbiota from *Rnls*<sup>+/+</sup> and *Rnls*<sup>-/-</sup> mice. Comparing to PBS group, fecal supernatant

from *Rnls*<sup>+/+</sup> mice elevated STC-1 cell proliferation more strongly after 48 h of co-culture, although there was also a significant difference was observed between *Rnls*<sup>-/-</sup> fecal supernatant group and PBS group. This result suggested that *Rnls* plays an important role in cell proliferation, possibly by remodeling the gut microbiota and their metabolites.

Metabolites, such as SCFAs, secondary bile acids, and serotonin or 5-HT, from microbiotas have been shown to influence glucose homeostasis<sup>35-38</sup>. Moreover, SCFAs and secondary bile acids also act on MAPK, Toll-like receptors, and Wnt and play different roles in cell growth, inflammation, and aging<sup>39,40</sup>. Reportedly, Akt/JNK signaling activation positively affects cell proliferation and metabolism<sup>41-43</sup>. Comparing to PBS group, fecal supernatants from *Rnls*<sup>+/+</sup> mice could effectively activate p-AKT no matter normalized to GAPDH or AKT, while there was only a significant difference of p-AKT was observed between *Rnls*<sup>-/-</sup> fecal supernatant group and PBS group normalized to AKT. Moreover, fecal supernatant from *Rnls*<sup>+/+</sup> mice exhibited higher expression of p-SAPK/JNK in comparison with fecal supernatant from *Rnls*<sup>-/-</sup> mice group and PBS

group. This finding suggested that *Rnls*<sup>-/-</sup> altered the microbiota-derived metabolites in the fecal supernatant, which led to the inactivation of p-AKT and p-SAPK/JNK and consequently lowered cell proliferation. In addition, several studies have demonstrated that *Rnls*, as a messenger, participates in acute injury and cancer progression<sup>24,44-47</sup>. With the consideration of these, our results suggest a novel character of *Rnls* in the maintenance of cellular homeostasis.

Metabolites from microbiota not only regulate cell growth but also participate in cell function. It has been shown that different performance in the gut microbiota alter the expression of *Pc1/3* in obesity-prone and obesity-resistant mice fed a high fat diet<sup>48</sup>. Moreover, the abundance of *Akkermansia muciniphila* is related to the secretory capacity of L cells<sup>14</sup>. The metabolites from *Bifidobacterium* and *Lactobacillus* have been identified that maintaining glucose homeostasis by altering the levels of several gut hormones through different signaling pathways<sup>49-51</sup>. Furthermore, a recent study demonstrated a decreased abundance of *Bifidobacterium* and *Lactobacillus* in *Rnls*<sup>-/-</sup> mice<sup>27</sup>. Therefore, we speculated that the changes in microbiota composition and metabolites by *Rnls* knockout could affect the expression of *Pc1/3*. Concordant with this hypothesis, our results demonstrated that fecal supernatant from *Rnls*<sup>+/+</sup> mice increased the mRNA expression of *Pc1/3*. Furthermore, the enzymatic hydrolysis activity of Boc-Arg-Val-Arg-Arg-MCA, a crucial factor affecting its function<sup>52</sup>, peaked after 12 h of fecal supernatant stimulation, and the fecal supernatants from *Rnls*<sup>+/+</sup> mice had a stronger effect on the increased the enzymatic hydrolysis activity of Boc-Arg-Val-Arg-Arg-MCA than the fecal supernatants from *Rnls*<sup>-/-</sup> mice. This result could be explained by the changed gut microbiota composition and microbiota derived metabolites owing to *Rnls* knockout, which might influence on the protein processing. However, to understand how these changes in the microbiota and its metabolites brought about by *Rnls* knockout affect protein processing, further studies are necessary. Briefly, using targeted metabolomics and metagenomics

analysis to uncover difference in metabolites from gut microbiota of *Rnls*<sup>+/+</sup> and *Rnls*<sup>-/-</sup> mice, following by the identification of differentially expressed genes and signaling pathways, particularly those genes and signaling pathway involved in organelles (endoplasmic reticulum and Golgi) associate to protein synthesis, processing. Finally, thorough the Bray-Curtis distance algorithm to calculate the effect of host and environmental factors on the alteration of genes and signaling pathways associated with endoplasmic reticulum and Golgi function.

Our results explore the possible way of *Rnls* effect on glucose metabolism and provide a novel perspective to understand the role of *Rnls* in T2D and the diagnosis, treatment of T2D. Although different behaviors were observed, there are some limitations to this study. First at all, one question is that the choice of cell line limited us exploring. The reasons why we chose STC-1 cell lines to mimic endocrine L cells function not native L cells could be explained as follows: 1) primary L-cells is difficult to culture and 2) STC-1 cell lines is frequently used as models to study endocrine L-cell physiology, 3) expresses higher *Pc1/3* than other L cell lines (GLUTag and NCI-H716 cell lines). What we were concerned with is the effect of microbiota metabolites on *Pc1/3* expression, so it is suitable to use STC-1 cell lines. However, there is a disadvantage of STC-1 cell lines. STC-1 cell lines expressed lower level GLP-2 and glicentin, it is very unfavorable for GLP-1 production<sup>53</sup>. GLP-1 is produced by the specific cleavage of proglucagon under the action of *Pc1/3*, meanwhile, the participation of GLP-2 and glicentin is necessary for GLP-1 production<sup>53</sup>. This is the one reason why we did not examine GLP-1 expression in this study. In further study, we will also use different type L cell lines to avoid such a disadvantage. Furthermore, owing to the purpose of this study is to analyze how the changes of metabolites in *Rnls*<sup>+/+</sup> and *Rnls*<sup>-/-</sup> mice influenced L cells function, we did not establish *Rnls* knockout L cell lines. Undoubtedly, establishing *Rnls* knockout L cell lines is good for understand the effect of *Rnls* on L cells activation directly. In further study, we will establish and use *Rnls*

knockout L cell lines or *Rnls* overexpression L cell lines to reveal the regulation of *Rnls* on L cells activation. Moreover, we will purify and quantify metabolites from fecal supernatants to provide a clearer view of their influence in future study. Another problem is that the stimulation time of fecal supernatant in vitro. As we all known, fecal supernatant concluded many metabolites, such as SCFAs, bile acids, lipopolysaccharide and so on<sup>16,17,54</sup>. Therefore, these metabolites how effect on cell activation behaves diversity<sup>16,17,54</sup>. Some in vitro studies analyzed the changes of cell activation happened at different times (4h to 48h)<sup>55-57</sup>. Hence, in this study, we chose 48h as the time point to analyze the changes of cell signaling. Of course, it is a little less rigorous. Analyzing changes in cell signaling pathways at different time periods or more earlier time periods are better to understand the changes of cell signaling pathway. We will pay more attention in further studies.

In summary, our study showed that *Rnls* knockout impairs the expression of Pc1/3 and the enzymatic hydrolysis activity of Boc-Arg-Val-Arg-Arg-MCA, which may accelerate glucose dysfunction progression by remodeling the gut microbiota and their metabolites.

### Conflicts of interest

The authors declare that they have no known competing financial interests or personal relationships that could have influenced the work reported in this study.

### Acknowledgements

This work was supported by the JST SPRING (grant number JPMJSP2124). In addition, we appreciated the English language editing by Editage (www.editage.jp).

### References

1. Ali MK, Pearson-Stuttard J, Selvin E and Gregg EW: Interpreting global trends in type 2 diabetes complications and mortality. *Diabetologia*, 65: 3–13, 2022.
2. Buse JB, Wexler DJ, Tsapas A, Rossing P, Mingrone G, Mathieu C, D'Alessio DA and Davies MJ: 2019 Update to: Management of Hyperglycemia in Type 2 Diabetes, 2018. A Consensus Report by the American Diabetes Association (ADA) and the European Association for the Study of Diabetes (EASD). *Diabetes Care*, 43: 487–493, 2020.
3. Taylor SI, Yazdi ZS and Beitelshes AL: Pharmacological treatment of hyperglycemia in type 2 diabetes. *J Clin Invest*, 131: e142243, 2021.
4. Gandhi GY and Mooradian AD: Management of Hyperglycemia in Older Adults with Type 2 Diabetes. *Drugs Aging*, 39: 39–58, 2022.
5. Ceriello A, Prattichizzo F, Phillip M, Hirsch IB, Mathieu C and Battelino T: Glycaemic management in diabetes: old and new approaches. *Lancet Diabetes Endocrinol*, 10: 75–84, 2022.
6. Piché ME, Tcherno A and Després JP: Obesity Phenotypes, Diabetes, and Cardiovascular Diseases. *Circ Res*, 126: 1477–1500, 2020.
7. Nieves-Cintrón M, Flores-Tamez VA, Le T, Baudel Martín-Aragón M and Navedo MF: Cellular and molecular effects of hyperglycemia on ion channels in vascular smooth muscle. *Cell Mol Life Sci*, 78: 31–61, 2021.
8. Greenwood M, Paterson A, Rahman PA, Gillard BT, Langley S, Iwasaki Y, Murphy D and Greenwood MP: Transcription factor Creb3l1 regulates the synthesis of prohormone convertase enzyme PC1/3 in endocrine cells. *J Neuroendocrinol*, 32: e12851, 2020.
9. Lafferty RA, O'Harte FPM, Irwin N, Gault VA and Flatt PR: Proglucagon-Derived Peptides as Therapeutics. *Front Endocrinol*, 12: 689678, 2021.
10. Ramzy A and Kieffer TJ: Altered islet prohormone processing: a cause or consequence of diabetes? *Physiol Rev*, 102: 155–208, 2022.
11. Moszak M, Szulińska M and Bogdański P: You Are What You Eat-The Relationship between Diet, Microbiota, and Metabolic Disorders-A Review. *Nutrients*, 12: 1096, 2020.
12. Tanase DM, Gosav EM, Neculae E et al.: Role of Gut Microbiota on Onset and Progression of Microvascular Complications of Type 2 Diabetes (T2DM). *Nutrients*, 12: 3719, 2020.
13. Wang PX, Deng XR, Zhang CH and Yuan HJ: Gut microbiota and metabolic syndrome. *Chin Med J*, 133: 808–816, 2020.
14. Everard A, Lazarevic V and Derrien M: Responses of gut microbiota and glucose and lipid metabolism to prebiotics in genetic obese and diet-induced leptin-

- resistant mice. *Diabetes*, 60: 2775–2786, 2011.
15. Wang Y, Dilidaxi D, Wu Y, Sailike J, Sun X and Nabi XH: Composite probiotics alleviate type 2 diabetes by regulating intestinal microbiota and inducing GLP-1 secretion in db/db mice. *Biomed Pharmacother*, 125: 109914, 2020.
  16. Kaji I, Karaki S and Kuwahara A: Short-chain fatty acid receptor and its contribution to glucagon-like peptide-1 release. *Digestion*, 89: 31–36, 2014.
  17. Tazoe H, Otomo Y, Kaji I, Tanaka R, Karaki SI and Kuwahara A: Roles of short-chain fatty acids receptors, GPR41 and GPR43 on colonic functions. *J Physiol Pharmacol*, 59 Suppl 2: 251–262, 2008.
  18. Benítez-Páez A, Hess AL, Krautbauer S, Liebisch G, Christensen L, Hjorth MF, TM, Sanz Y and Consortium MNG: Sex, Food, and the Gut Microbiota: Disparate Response to Caloric Restriction Diet with Fiber Supplementation in Women and Men. *Mol Nutr Food Res*, 65: e2000996, 2021.
  19. Suzuki TA and Ley RE: The role of the microbiota in human genetic adaptation. *Science*, 370: eaaz6827, 2020.
  20. Xu J, Li G, Wang P, Velazquez H, Yao X and Li Y, Wu Y, Peixoto A, Crowley S and Desir GV: Renalase is a novel, soluble monoamine oxidase that regulates cardiac function and blood pressure. *J Clin Invest*, 115: 1275–1280, 2005.
  21. Buraczynska M, Gwiazda-Tyndel K, Drop B and Zaluska W : Renalase gene Glu37Asp polymorphism affects susceptibility to diabetic retinopathy in type 2 diabetes mellitus. *Acta Diabetol*, 58: 1595–1602, 2021.
  22. Czubilińska-ŁJ, Gliwińska A, Badeński A and Szczepańska M: Associations between renalase concentration and the occurrence of selected diseases. *Endokrynol Pol*, 71: 334–342, 2020.
  23. Zhang F, Liu W, Wu Y, Li X, Zhang S, Feng Y, Lu R and Sun L: Association of renalase gene polymorphisms with the risk of hypertensive disorders of pregnancy in northeastern Han Chinese population. *Gynecol Endocrinol*, 36: 986–990, 2020.
  24. Pointer TC, Gorelick FS and Desir GV: Renalase: A Multi-Functional Signaling Molecule with Roles in Gastrointestinal Disease. *Cells*, 10: 2006, 2021.
  25. Tokinoya K, Sekine N, Aoki K, Ono S, Kuji T, Sugawara T, Yoshida Y and Takekoshi K: Effects of renalase deficiency on liver fibrosis markers in a nonalcoholic steatohepatitis mouse model. *Mol Med Rep*, 23: 210, 2021.
  26. Aoki K, Yanazawa K, Tokinoya K, Sugawara T, Suzuki T, Yoshida Y, Nakano T, Omi N, Kawakami Y and Takekoshi K: Renalase is localized to the small intestine crypt and expressed upon the activation of NF- $\kappa$ B p65 in mice model of fasting-induced oxidative stress. *Life Sci*, 267: 118904, 2021.
  27. Fang H, Aoki K, Tokinoya K, Yonamine M, Sugawara T, Kawakami Y and Takekoshi K: Effects of High-Fat Diet on the Gut Microbiota of Renalase Gene Knockout Mice. *Obesities*, 2: 303–316, 2022.
  28. Singh P, Grabauskas G, Zhou S, Gao J, Zhang Y and Owyang C: High FODMAP diet causes barrier loss via lipopolysaccharide-mediated mast cell activation. *JCI Insight*, 6: e146529 2021.
  29. Meelu P, Marin R, Clish C, Zella G, Cox S, Yajnik V, Nguyen DD and Korzenik JR: Impaired innate immune function associated with fecal supernatant from Crohn’s disease patients: insights into potential pathogenic role of the microbiome. *Inflamm Bowel Dis*, 20: 1139–1146, 2014.
  30. Sugawara T, Mukai N, Tamura K et al: Effects of Cold Stimulation on Mitochondrial Activity and VEGF Expression in vitro. *Int J Sports Med*, 37: 766–778, 2016.
  31. Azaryan AV, Krieger TJ and Hook VY: Purification and characteristics of the candidate prohormone processing proteases PC2 and PC1/3 from bovine adrenal medulla chromaffin granules. *J Biol Chem*, 270: 8201–8208, 1995.
  32. Magne F, Gotteland M, Gauthier L, Zazueta A, Pessoa S, Navarrete P and Balamurugan R: The Firmicutes/Bacteroidetes Ratio: A Relevant Marker of Gut Dysbiosis in Obese Patients? *Nutrients*, 12: 1474, 2020.
  33. Bo TB, Wen J, Zhao YC, Tian SJ, Zhang XY and Wang DH: Bifidobacterium pseudolongum reduces triglycerides by modulating gut microbiota in mice fed high-fat food. *J Steroid Biochem Mol Biol*, 198: 105602, 2020.
  34. Zhang Q, Hu J, Feng JW et al: Influenza infection elicits an expansion of gut population of endogenous Bifidobacterium animalis which protects mice against infection. *Genome Biol*, 21: 99, 2020.
  35. Zhang HY, Tian JX, Lian FM, Li M, Liu WK, Zhen Z, Liao JQ and Tong XL: Therapeutic mechanisms of traditional Chinese medicine to improve metabolic diseases via the gut microbiota. *Biomed Pharmacother*, 133: 110857, 2021.
  36. Kaska L, Sledzinski T, Chomiczewska A, Dettlaff-Pokora A and Swierczynski J: Improved glucose metabolism following bariatric surgery is associated with increased circulating bile acid concentrations and remodeling of the gut microbiome. *World J*

- Gastroenterol, 22: 8698–8719, 2016.
37. Sun L, Pang Y, Wang X, Wu Q, Liu H, Liu B, Liu G, Ye M, Kong W and Jiang C: Ablation of gut microbiota alleviates obesity-induced hepatic steatosis and glucose intolerance by modulating bile acid metabolism in hamsters. *Acta Pharm Sin B*, 9: 702–710, 2019.
  38. Tveter KM, Villa-Rodriguez JA, Cabales AJ, Zhang L, Bawagan FG, Duran RM and Roopchand DE: Polyphenol-induced improvements in glucose metabolism are associated with bile acid signaling to intestinal farnesoid X receptor. *BMJ Open Diabetes Res Care*, 8: e001386, 2020.
  39. Spor A, Koren O and Ley R: Unravelling the effects of the environment and host genotype on the gut microbiome. *Nat Rev Microbiol*, 9: 279–290, 2011.
  40. De Angelis M, Garruti G, Minervini F, Bonfrate L, Portincasa P and Gobetti M: The Food-gut Human Axis: The Effects of Diet on Gut Microbiota and Metabolome. *Curr Med Chem*, 26: 3567–3583, 2019.
  41. Wang H, Chinnathambi A, Alahmadi TA, Alharbi SA, Veeraraghavan VP, Mohan SK, Hussain S, Ramamoorthy K and Rengarajan T: Phyllanthin inhibits MOLT-4 leukemic cancer cell growth and induces apoptosis through the inhibition of AKT and JNK signaling pathway. *J Biochem Mol Toxicol*, 35: 1–10, 2021.
  42. Zheng B, Zheng Y, Zhang N, Zhang Y and Zheng B: Rhoifolin from *Plumula Nelumbinis* exhibits anti-cancer effects in pancreatic cancer via AKT/JNK signaling pathways. *Sci Rep*, 12: 5654, 2022.
  43. Zhao L, Xue M, Zhang L et al: MicroRNA-4268 inhibits cell proliferation via AKT/JNK signalling pathways by targeting Rab6B in human gastric cancer. *Cancer Gene Ther*, 27: 461–472, 2020.
  44. Wang L, Velazquez H, Moeckel G, Chang J, Ham A, Lee HT, Safirstein R and Desir GV: Renalase prevents AKI independent of amine oxidase activity. *J Am Soc Nephrol*, 25: 1226–1235, 2014.
  45. Wu Y, Quan C, Yang Y, Liang Z, Jiang W and Li X: Renalase improves pressure overload-induced heart failure in rats by regulating extracellular signal-regulated protein kinase 1/2 signaling. *Hypertens Res*, 44: 481–488, 2021.
  46. Guo X, Hollander L, MacPherson D, Wang L, Velazquez H, Chang J, Safirstein R, Cha C, Gorelick F and Desir GV: Inhibition of renalase expression and signaling has antitumor activity in pancreatic cancer. *Sci Rep*, 6: 22996, 2016.
  47. Zhang T, Gu J, Guo J, Chen K, Li H and Wang J: Renalase attenuates mouse fatty liver ischemia/reperfusion injury through mitigating oxidative stress and mitochondrial damage via activating SIRT1. *Oxid Med Cell Longev*, 2019: 7534285, 2019.
  48. Razolli DS, De Araújo TM, Sant Apos Ana MR, Kirwan P, Cintra DE, Merkle FT and Velloso LA: Proopiomelanocortin processing in the hypothalamus is directly regulated by saturated fat: Implications for the development of obesity. *Neuroendocrinology*, 110: 92–104, 2020.
  49. Tolhurst G, Heffron H, Lam YS, Parker HE, Habib AM, Diakogiannaki E, Cameron J, Grosse J, Reimann F and Gribble FM: Short-chain fatty acids stimulate glucagon-like peptide-1 secretion via the G-protein-coupled receptor FFAR2. *Diabetes*, 61: 364–371, 2012.
  50. Scott KP, Gratz SW, Sheridan PO, Flint HJ and Duncan SH: The influence of diet on the gut microbiota. *Pharmacol Res*, 69: 52–60, 2013.
  51. Charrier JA, Martin RJ, McCutcheon KL et al: High fat diet partially attenuates fermentation responses in rats fed resistant starch from high-amylose maize. *Obesity (Silver Spring)*, 21: 2350–2355, 2013.
  52. Hoshino A, Kowalska D, Jean F, Lazure C and Lindberg I: Modulation of PC1/3 activity by self-interaction and substrate binding. *Endocrinology*, 152: 1402–1411, 2011.
  53. Rune EK, Nicolai Jacob WA, Carolyn FD, Emilie BM, Jens FR, Frank R, Fiona MG and Jens JH: Peptide production and secretion in GLUTag, NCI-H716 and STC-1 cells: a comparison to native L-cells. *J Mol Endocrinol*, 56: 201–211, 2016.
  54. Han H, Yi B, Zhong RQ, Wang MY, Zhang SF, Ma J, Yin YL, Yin J, Chen Land Zhang HF: From gut microbiota to host appetite: gut microbiota-derived metabolites as key regulators. *Microbiome*, 9: 162, 2021.
  55. Mari LL; Giovanni S; Kristoffer LE et al: L-Cell Differentiation Is Induced by Bile Acids Through GPBAR1 and Paracrine GLP-1 and Serotonin Signaling. *Diabetes*, 69: 614–623, 2020.
  56. Qin LS, Yao WL, Wang TX, Jin TM, Guo BY, Wen S and Huang FR: Targeting gut microbiota derived butyrate improves hepatic gluconeogenesis through the cAMP-PKA-GCN5 pathway in late pregnant sows. *Food Funct*, 13: 4360–4374, 2022.
  57. Besten GD, Bleeker A, Gerding A et al: Short-chain fatty acids protect against high-fat diet-induced obesity via a PPAR $\gamma$ -dependent switch from lipogenesis to fat Oxidation. *Diabetes*, 64: 2398–2408, 2015.